

# A THEORETICAL STUDY OF PULMONARY CAPILLARY GAS EXCHANGE AND VENOUS ADMIXTURE

HOWARD T. MILHORN, JR. *and* PAUL E. PULLEY, JR.

*From the Biomedical Engineering Section of the Department of Physiology and Biophysics and the Computer Center of the University of Mississippi School of Medicine, Jackson, Mississippi 39216*

**ABSTRACT** A model of pulmonary capillary gas exchange and venous admixture is presented and the inclusion of this model into a model of the entire respiratory system is discussed. Partial pressure and concentration gradients for nitrogen, helium, oxygen, and carbon dioxide are predicted. The cases of breathing room air and 10% oxygen are studied. In both of these studies the Bohr and Haldane effects are included, and the "physiological" dissociation curves of oxygen and carbon dioxide are predicted for the normal case as blood flows from the venous blood end of the capillary to the arterial blood end. Venous admixture effects are also calculated for both of these cases. The effects of emphysema, pulmonary congestion, and altered cardiac function on the gradients are studied.

## INTRODUCTION

As blood flows along the pulmonary capillaries, it receives oxygen from the alveoli and delivers carbon dioxide to them. Thus, concentration gradients for these two gases develop along the pulmonary capillaries, increasing for oxygen and decreasing for carbon dioxide. Several factors, such as cardiac output, pulmonary membrane area and thickness, and blood combining power determine the exact shape of the gradient curves, and hence the partial pressure differences between alveolar gas and end capillary blood gas. Carbon dioxide, having a diffusion coefficient about 20 times that of oxygen, diffuses much more rapidly so that equilibrium is thought to be invariably reached, regardless of changes in these factors. Oxygen equilibrium, however, is thought to be limited either by blood flow or diffusion under certain conditions. In the flow-limiting situation, cardiac output is too great to allow equilibration of alveolar and blood oxygen partial pressures. In the diffusion limiting situation, the pulmonary membrane, perhaps owing to a disease state such as emphysema or pulmonary congestion, is pathologically altered so that diffusion occurs too slowly to allow equilibrium to be reached between alveolar gas and blood

gas. Both cases (that is, flow and diffusion limitation) may of course occur simultaneously.

As blood passes out of the pulmonary capillaries, it mixes with blood which has bypassed the capillaries so that the partial pressures of arterial blood gases are different from those of end alveolar capillary blood. This effect is the venous admixture phenomenon.

The purpose of this paper is to develop a theoretical model of pulmonary capillary gas exchange and venous admixture so that it can later be incorporated into a complete digital computer model of the human respiratory system. Previous attempts at simulating respiratory phenomena (Grodins et al., 1954; Defares et al., 1960; Horgan and Lange, 1962; Milhorn and Guyton, 1965; Milhorn et al., 1965; Milhorn and Guyton, 1966; Longobardo et al., 1966; Milhorn et al., 1967) have all assumed that alveolar capillary partial pressures reach equilibrium with alveolar gases or have used a simple approximation to account for the alveolar-arterial partial pressure difference. This approximation has included a lumped combination of both flow and diffusion limitation and venous admixture effects. The theoretical analysis which is to follow will investigate the relative importance of each of these factors separately under several conditions.

Before actually investigating the nonlinear case of oxygen and carbon dioxide, however, we will take a look at the simpler linear case of the inert gases, nitrogen and helium.

The basic concept of the development of the equations which is to follow is based upon the well known Bohr graphic integration technique and is an extension of the work by Defares and Visser in 1962.

#### DERIVATION OF EQUATIONS

Fig. 1 shows a schematic diagram of the pulmonary system. Blood enters the pulmonary system at a rate  $\dot{Q}$  and carries a gas of concentration  $C_v$ . The blood flow then splits, the major portion passing through the pulmonary capillaries where it exchanges gases with the alveoli. A small part of the blood flow, however, bypasses the capillaries and returns to the arterial blood, thereby causing the venous admix-

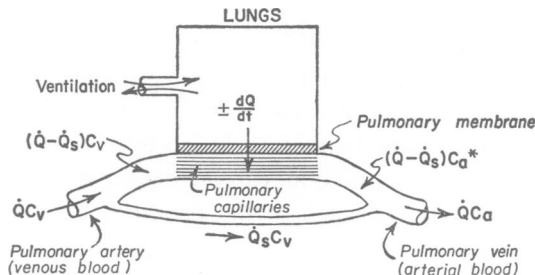


FIGURE 1 The pulmonary system.

ture effect. In actuality, the venous admixture effect results from (a) true arterio-venous (a-v) anastomoses, (b) the bronchial veins which drain into the pulmonary veins, (c) the thebesian veins which return some blood from the myocardium to the left ventricle, and (d) a nonuniform ventilation/perfusion ratio. In this study we will lump all of these factors together and treat them as a-v shunts.

The following symbols will be used in deriving the equations of capillary gas exchange and venous admixture in the pulmonary system of Fig. 1. The subscript O<sub>2</sub> will be added when referring to oxygen, CO<sub>2</sub> for carbon dioxide, N<sub>2</sub> for nitrogen, and He<sub>2</sub> for helium.

$P_A$	alveolar gas partial pressure (mm Hg)
$P_v$	venous blood gas partial pressure (mm Hg)
$P_a^*$	end alveolar capillary gas partial pressure (mm Hg)
$P_a$	arterial gas partial pressure (mm Hg)
$P$	partial pressure of gas at any point along the pulmonary "capillary" (mm Hg)
$P_B$	barometric pressure (mm Hg)
$(\Delta P)_{av}$	average partial pressure difference between gas in alveolus and in pulmonary capillary blood (mm Hg)
$C_v$	venous blood gas concentration (dimensionless)
$C_a^*$	end pulmonary capillary gas concentration (dimensionless)
$C_a$	arterial gas concentration (dimensionless)
$C$	concentration of blood gas at any point along the pulmonary "capillary" (dimensionless)
$\dot{Q}$	cardiac output (liters/min)
$\dot{Q}_s$	pulmonary shunt flow (liters/min)
$\delta$	fraction of $\dot{Q}$ which is $\dot{Q}_s$ ; i.e., $\dot{Q}_s/\dot{Q}$ (dimensionless)
$\alpha$	solubility coefficient (atm <sup>-1</sup> )
$dQ_{O_2}/dt$	net rate of diffusion of oxygen across the pulmonary membrane (liters/min)
$F_1(P_{O_2}, P_{CO_2})$	expression of the oxygen dissociation curve of whole blood
$F_2(P_{CO_2}, P_{O_2})$	expression of the carbon dioxide dissociation curve of whole blood
$dq/dt$	net rate of diffusion of a gas into or out of the small cylinder shaped element of Fig. 2 (liters/min)
$f$	blood flow through a single pulmonary "capillary" (liters/min)
$r$	radius of a pulmonary "capillary" (meters)
$x_a$	length of a pulmonary "capillary" (meters)
$x$	distance from venous blood end of "capillary" to any point along the "capillary" (meters)
$n$	number of equivalent pulmonary "capillaries" (dimensionless)
$T_m$	effective pulmonary membrane thickness (meters)

$A$	total pulmonary capillary surface area available for diffusion (meters <sup>2</sup> )
$K$	constant which depends upon the physical structure of the pulmonary membrane ( $\text{kg}^{1/2}\text{-liters-atm/min-meters}$ )
$MW$	molecular weight (kilograms)
$\dot{V}$	oxygen consumption or carbon dioxide production rate (liters/min)
$D_c$	diffusing capacity of the thin cylinder of Fig. 2 (liters/min/mm Hg)
$D$	total diffusing capacity (liters/min/mm Hg)
$\beta$	arbitrary constant which varies from zero at the venous blood end of pulmonary capillary to unity at the arterial blood end (dimensionless)

### *The Pulmonary Capillary Gas Exchange Equations*

The capillary system of the lungs has been shown to consist of a complex hexagonal network (Weibel and Gomez, 1962). As is often done in electrical network theory, an equivalent parallel network will be assumed in this study. The dimensions of these hypothetical capillaries will, of course, bear no resemblance to the actual dimensions. In the evolution of the final set of equations, these dimensions will be eliminated so that they will be of no consequence in the final model.

Fig. 2 shows a schematic diagram of one of the hypothetical pulmonary capillaries. The net rate of flow of a gas across the surface area of the thin cylinder can be expressed as

$$\frac{dq}{dt} = D_c(P_A - P), \quad (1)$$

where  $dP$  has been ignored, since  $dP \ll P$ . In this equation,  $P_A$  is the alveolar partial pressure,  $P$  is the partial pressure within the blood of the cylinder, and  $D_c$  is the diffusing capacity (transfer coefficient) of the membrane which makes up the surface of the cylinder. In actuality, the diffusing capacity is composed of two com-

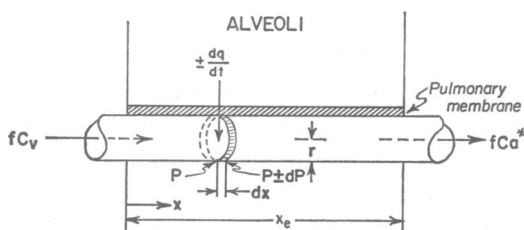


FIGURE 2 A single pulmonary capillary.

ponents; i.e., the pulmonary membrane transfer coefficient and the transfer coefficient (reaction velocity) of the red blood cell. In this study we will consider the total diffusing capacity and not concern ourselves with its components.

The diffusing capacity of the cylinder can be expressed as a combination of factors as follows:

$$D_c = K \left( \frac{2\pi r dx}{T_m} \right) \left( \frac{\alpha/P_B}{(MW)^{1/2}} \right). \quad (2)$$

In this equation,  $K$  is a constant whose value depends upon the physicochemical structure of the membranes involved,  $2\pi r dx$  is the surface area of the cylinder,  $T_m$  is the effective membrane thickness (diffusing distance),  $\alpha/P_B$  is the solubility coefficient expressed in mm Hg<sup>-1</sup>, and MW is the molecular weight of the gas involved. The ratio  $(\alpha/P_B)/(MW)^{1/2}$  is proportional to the diffusion coefficient which determines the rate of diffusion per mm Hg pressure difference for each gas.

Combining equations 1 and 2, we obtain

$$\frac{dq}{dt} = K \left( \frac{2\pi r dx}{T_m} \right) \left( \frac{\alpha/P_B}{(MW)^{1/2}} \right) (P_A - P). \quad (3)$$

According to the law of mass balance (Fick principle), the net rate of flow of gas across the cylinder must be equal to the blood flow  $f$ , times the blood gas concentration difference  $dC$  between the ends of the cylinder. Hence

$$\frac{dq}{dt} = f dC. \quad (4)$$

Setting the right hand side of equation 4 equal to the right hand side of equation 3, rearranging, and integrating both sides yields

$$\int_{c_v}^c \left( \frac{1}{P_A - P} \right) dC = K \frac{2\pi r \alpha / P_B}{f T_m (MW)^{1/2}} \int_0^x dx = K \frac{2\pi r \alpha / P_B}{f T_m (MW)^{1/2}} x. \quad (5)$$

Examining equation 5, we see that it contains the hypothetical quantities  $r$ ,  $x$ , and  $f$ . We must now eliminate these. This can be done as follows: The total number of parallel "capillaries"  $n$ , can be expressed as

$$n = (\dot{Q} - \dot{Q}_s) / f. \quad (6)$$

The total capillary surface area  $A$  available for diffusion is

$$A = (2\pi r x_s) n. \quad (7)$$

Combining equations 6 and 7, eliminating  $n$ , and solving for  $x_s$  yields

$$x_s = \frac{Af}{2\pi r (\dot{Q} - \dot{Q}_s)} \quad (8)$$

If we define an arbitrary constant  $\beta$  such that  $0 \leq \beta \leq 1$ , we can write the distance from the venous blood end  $x$  along the capillary path as

$$x = \beta x_s \quad (9)$$

where  $\beta$  is zero at the venous blood end and unity at the arterial blood end.

Combining equations 8 and 9 yields

$$x = \beta \frac{Af}{2\pi r(\dot{Q} - \dot{Q}_s)} = \beta \frac{Af}{2\pi r\dot{Q}(1 - \delta)}, \quad (10)$$

in which  $\delta$  is the fraction of  $\dot{Q}$  which is  $\dot{Q}_s$ ; i.e.,  $\dot{Q}_s/\dot{Q}$ .

Substituting equation 10 into equation 5 yields the general equation of pulmonary capillary gas exchange:

$$\int_{C_v}^C \left( \frac{1}{P_A - P} \right) dC = \beta \left( K \frac{A}{T_m} \right) \frac{\alpha/P_B}{(MW)^{1/2}\dot{Q}(1 - \delta)}, \quad (11)$$

in which the constant  $(KA/T_m)$  is composed of three membrane factors,  $K$ ,  $A$ , and  $T_m$ . It should be noted that the unknown hypothetical quantities ( $r$ ,  $x$ ,  $f$ ) have successfully been eliminated.

For a particular gas, all constants in the right hand side of equation 11 have values which are well substantiated, except for the membrane constant  $(KA/T_m)$ . The value of this factor must, therefore, be determined. This is done as follows: The total net rate of diffusion of oxygen  $dQ_{O_2}/dt$  across the entire pulmonary membrane can be expressed as

$$\frac{dQ_{O_2}}{dt} = \left( K \frac{A}{T_m} \right) \left( \frac{\alpha_{O_2}/P_B}{(MW_{O_2})^{1/2}} \right) (\Delta P_{O_2})_{av}, \quad (12)$$

in which  $(\Delta P_{O_2})_{av}$  is the average pressure difference between alveolus and pulmonary capillary blood.

Solving equation 12 for  $(KA/T_m)$  yields

$$K \frac{A}{T_m} = \frac{(dQ_{O_2}/dt)(MW_{O_2})^{1/2}}{(\alpha_{O_2}/P_B)(\Delta P_{O_2})_{av}}. \quad (13)$$

In the steady state,  $dQ_{O_2}/dt$  is equal to oxygen consumption  $\dot{V}_{O_2}$  and  $(\Delta P_{O_2})_{av}$  can be expressed as  $\dot{V}_{O_2}/D_{O_2}$  where  $D_{O_2}$  is the diffusing capacity of oxygen. Substituting these relationships into equation 13 yields

$$K \frac{A}{T_m} = \left[ \frac{(MW_{O_2})^{1/2}}{\alpha_{O_2}/P_B} \right] D_{O_2}. \quad (14)$$

All of the terms on the right hand side of equation 14 have values which are well substantiated so that  $(KA/T_m)$  can now be determined.

Substitution of  $MW_{O_2} = 0.032 \text{ kg}$ ,  $\alpha_{O_2} = 0.022 \text{ atm}^{-1}$ ,  $P_B = 760 \text{ mm Hg}$ , and  $D_{O_2} = 0.021 \text{ liters/min/mm Hg}$  yields a value of 129.3 for  $KA/T_m$ .  $K$  is therefore

$$K = (129.3)/(T_m/A).$$

Values of  $T_m = 0.5 \times 10^{-6} \text{ m}$  and  $A = 70 \text{ m}^2$  yield a numerical value for  $K$  of approximately  $9.2 \times 10^{-7}$ . The reason for separating  $KA/T_m$  is so that  $A/T_m$  can be maintained as a variable parameter in the final set of equations. Since the entire term  $KA/T_m$  will appear in the final equation, accuracy is not impaired in the slightest by using approximate values of  $A$  and  $T_m$ . Any error in the estimation of these values will be corrected by the determined value of  $K$ .

Determination of  $KA/T_m$  by the preceding manner insures that we have included diffusion across the pulmonary membrane, through the plasma, and across the red cell membrane in the model. We have made the assumption, however, that at the molecular site, combination with hemoglobin is instantaneous.

Referring to equation 11, it can be seen that a solution for the gradient along the pulmonary capillary pathway could now be obtained by incrementing  $\beta$  in small steps from zero to unity, provided we had a relationship between partial pressure  $P$  and concentration  $C$ . This relationship is, of course, the respective blood dissociation curve.

Using equation 14, changing the limits of the integral of equation 11 to partial pressures, and rearranging the right hand side, the general equation of pulmonary capillary gas exchange in terms of partial pressure becomes

$$\int_{P_v}^P \left( \frac{1}{P_A - P} \right) dF(P) = \beta K \left( \frac{A}{T_m \dot{Q}} \right) \frac{\alpha/P_B}{(MW)^{1/2}(1 - \delta)}, \quad (15)$$

in which  $F(P)$  denotes the function of partial pressure related to the concentration of the respective gas under study. It should be noted that for a given gas, all the factors in the right hand side of equation 15 are fixed, with the exception of the term  $A/T_m \dot{Q}$ . This means that the capillary gradients can be altered by changes in surface area, membrane thickness, cardiac output, or any combination of the three. We will return to this equation later in the paper.

### *The Venous Admixture Equations*

Now, let us consider the venous admixture problem. By reference to Fig. 1, it is seen that the rate at which gas enters the pulmonary vein  $\dot{Q}C_a$  can be expressed as

$$\dot{Q}C_a = (\dot{Q} - \dot{Q}_s)C_a^* + \dot{Q}_s C_v, \quad (16)$$

or dividing by  $\dot{Q}$  and using the relationship  $\dot{Q}_s/\dot{Q} = \delta$

$$C_a = (1 - \delta)C_a^* + \delta C_v \quad (17)$$

In equation 17,  $C_a$  can be converted to partial pressure by making use of the blood dissociation curve of the particular gas under study. This will be done later in the paper.

Equations 15 and 17 are the general equations of pulmonary capillary gas exchange and venous admixture. We will adapt these for (a) the linear case of nitrogen and helium and (b) the nonlinear case of oxygen and carbon dioxide.

To solve for a numerical value of the ratio  $\delta$ , we solve equation 16 for  $\dot{Q}_s/\dot{Q}$  as follows:

$$\frac{\dot{Q}_s}{\dot{Q}} = \left[ \frac{C_v - C_a^*}{C_a - C_a^*} \right] = \delta. \quad (18)$$

To evaluate the term in the brackets, let us consider the special case of oxygen. Hence

$$\delta = \left[ \frac{C_{vO_2} - C_{aO_2}^*}{C_{aO_2} - C_{aO_2}^*} \right], \quad (19)$$

or switching to partial pressures

$$\delta = \left[ \frac{F_1(P_{vO_2}, P_{vCO_2}) - F_1(P_{aO_2}^*, P_{aCO_2}^*)}{F_1(P_{aO_2}, P_{aCO_2}) - F_1(P_{aO_2}^*, P_{aCO_2}^*)} \right]. \quad (20)$$

Using normal values of  $P_{vO_2} = 40$ ,  $P_{vCO_2} = 46$ ,  $P_{aO_2}^* = 104$ ,  $P_{aCO_2}^* = 40$ ,  $P_{aO_2} = 97$ , and  $P_{aCO_2} = 40$ , and an empirical function  $F_1$  which will be discussed later, a value of 0.013 was determined for  $\delta$ . This means that in the normal situation, effective pulmonary a-v shunt flow is 1.3 per cent of cardiac output.

#### THE LINEAR CASE: N<sub>2</sub> AND HE<sub>2</sub>

In the system under study, linearity depends upon whether the relationship between concentration and partial pressure in blood of the particular gas under study is linear or nonlinear. The oxygen and carbon dioxide dissociation curves of whole blood are clearly nonlinear. Furthermore, the situation is further complicated by the Bohr and Haldane effects. These effects, coupled with the nonlinear dissociation curves, make the O<sub>2</sub>-CO<sub>2</sub> system a difficult one to study. The linear case of inert gases is a simpler one to study because (a) inert gases obey Henry's law in blood which is linear and (b) there is no coupling with a second gas as in the O<sub>2</sub>-CO<sub>2</sub> case. Therefore, we will consider the linear case first.

In developing the solution for the linear case we will solve equation 15 in general for any inert gas. We will then adapt it for nitrogen and helium, the two inert gases which are of importance in different aspects of respiratory physiology.

For the linear case, the gas under study obeys Henry's law in blood; i.e.

$$C = (\alpha/P_B)P, \quad (21)$$



in which  $C$  is concentration,  $P$  is partial pressure,  $\alpha$  is the solubility coefficient, and  $P_B$  is barometric pressure. Therefore, substituting equation 21 into equation 15, we obtain

$$\int_{P_v}^P \left( \frac{1}{P_A - P} \right) dP = \beta K \left( \frac{A}{T_m \dot{Q}} \right) / (MW)^{1/2} (1 - \delta). \quad (22)$$

Integration of equation 22 yields

$$\log_e \left( \frac{P_A - P}{P_A - P_v} \right) = -\beta K \left( \frac{A}{T_m \dot{Q}} \right) / (MW)^{1/2} (1 - \delta). \quad (23)$$

Taking the exponential of each side and rearranging we obtain our desired solution

$$P = P_A - (P_A - P_v) \exp \left[ -\beta K \left( \frac{A}{T_m \dot{Q}} \right) / (MW)^{1/2} (1 - \delta) \right]. \quad (24)$$

Using equation 21, equation 17 can be written in terms of partial pressure as

$$P_a = (1 - \delta) P_a^* + \delta P_v. \quad (25)$$

Equations 24 and 25 describe the diffusion and venous admixture effects of inert gases in the pulmonary system. When these are written specifically for nitrogen and helium they become

$$P_{N_2} = P_{AN_2} - (P_{AN_2} - P_{vN_2}) \exp \left[ -\beta K \left( \frac{A}{T_m \dot{Q}} \right) / (MW_{N_2})^{1/2} (1 - \delta) \right], \quad (26)$$

$$P_{aN_2} = (1 - \delta) P_{aN_2}^* + \delta P_{vN_2}, \quad (27)$$

$$P_{He_2} = P_{AHe_2} - (P_{AHe_2} - P_{vHe_2}) \exp \left[ -\beta K \left( \frac{A}{T_m \dot{Q}} \right) / (MW_{He_2})^{1/2} (1 - \delta) \right], \quad (28)$$

$$P_{aHe_2} = (1 - \delta) P_{aHe_2}^* + \delta P_{vHe_2}. \quad (29)$$

Although the actual gradients for  $N_2$  and  $He_2$  are unrelated, we will consider them together. Our procedure is equivalent to suddenly replacing half of the inspired nitrogen with helium and studying the results on gas exchange and venous admixture at desired points of time.

The values of parameters used in this model which hold for any gas and which will be used again later for the nonlinear cases are:

$$\begin{array}{ll} 0 \leq \beta \leq 1 \text{ (dimensionless)} & K = 9.2 \times 10^{-7} \text{ (kg}^{1/2}\text{-liters-atm/min-meters)} \\ \dot{Q} = 5.3 \text{ liters/min} & A = 70 \text{ (m}^2\text{)} \\ \delta = 0.013 \text{ (dimensionless)} & T_m = 0.5 \times 10^{-6} \text{ (m)} \end{array}$$

The values of parameters used which pertain to the single study of inert gases which is to follow are:

$$\begin{array}{ll}
 P_{AN_2} = 284.5 \text{ mm Hg} & P_{vHe_2} = 0.0 \text{ mm Hg} \\
 P_{vN_2} = 569.0 \text{ mm Hg} & MW_{He_2} = 0.008 \text{ kg.} \\
 MW_{N_2} = 0.012 \text{ kg} & \alpha_{N_2} = 0.0147 \text{ (atm}^{-1}\text{)} \\
 P_{AHe_2} = 284.5 \text{ mm Hg} & \alpha_{He_2} = 0.0094 \text{ (atm}^{-1}\text{)}
 \end{array}$$

Partial pressure gradients for helium and nitrogen are shown in Fig. 3 for  $P_{AN_2} = 284.5$ ,  $P_{AHe_2} = 284.5$ ,  $P_{vN_2} = 569.0$ , and  $P_{vHe_2} = 0$ . Although alveolar and blood partial pressures theoretically never reach equilibrium, for the purposes of dis-

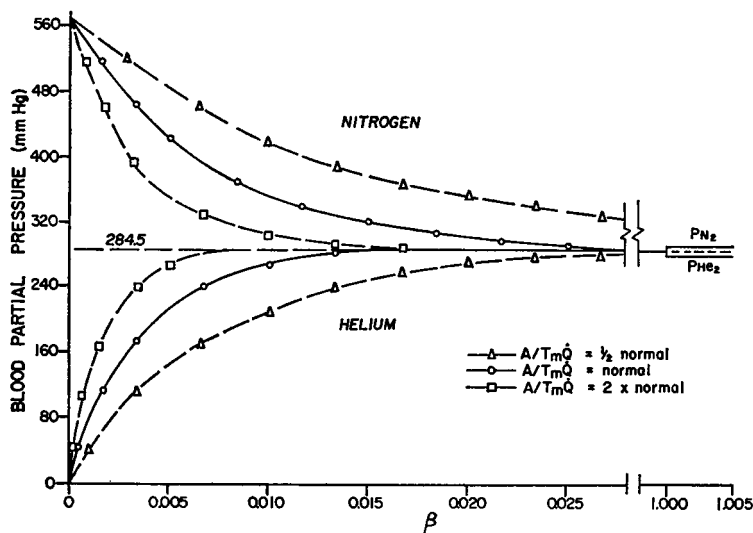


FIGURE 3 Nitrogen and helium partial pressure gradients along the pulmonary capillary pathway and venous admixture effects for  $P_{AN_2} = 284.5$ ,  $P_{AHe_2} = 284.5$ ,  $P_{vN_2} = 569.0$ , and  $P_{vHe_2} = 0$ .

cussion in this paper we will define equilibrium to mean the point at which the alveolar-blood difference becomes less than 0.1% of the maximum difference. Note that equilibrium of alveolar and blood gases occurs very quickly. This is because of the small quantity of inert gas required to cause large changes in the blood partial pressure as can be calculated from equation 21. The curve for the normal value of  $A/T_m\dot{Q}$  is marked by the circles, the situation in which  $A/T_m\dot{Q}$  is reduced to one-half normal is marked by squares, and the situation in which  $A/T_m\dot{Q}$  is increased to two times normal is marked by the triangles. Venous admixture effects are shown at  $\beta = 1.0$ . Arterial  $P_{He_2}$  drops from 284.5 mm Hg to 281.1 and  $P_{N_2}$  rises from 284.5 mm Hg to 288.5.

Concentration gradients for helium and nitrogen are shown in Fig. 4 for the values

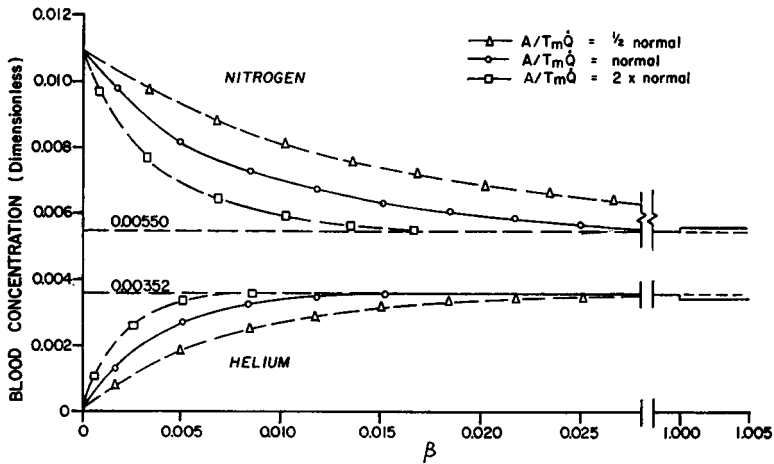


FIGURE 4 Nitrogen and helium concentration gradients along the pulmonary capillary pathway and venous admixture effects for the values given in Fig. 3.

of parameters given in Fig. 3. Note the very small concentration changes which occur corresponding to the large partial pressure changes. Again, venous admixture effects are shown at  $\beta = 1.0$ . Arterial  $C_{\text{He}_2}$  drops from 0.00352 to 0.00348 and  $C_{\text{N}_2}$  rises from 0.00550 to 0.00558.

### THE NONLINEAR CASE: $\text{O}_2$ AND $\text{CO}_2$

Let us now turn our attention to the nonlinear case; i.e., the case of oxygen and carbon dioxide. The equations for capillary gas exchange are nonlinear for this case because of the nonlinear  $\text{O}_2$  and  $\text{CO}_2$  dissociation curves of blood. The situation is further complicated by the fact that these curves are dependent upon each other. The  $P_{\text{CO}_2}$  affects the oxygen dissociation curve (Bohr effect) and  $P_{\text{O}_2}$  affects the carbon dioxide dissociation curve (Haldane effect). We will include both of these effects in our analysis of the nonlinear case.

Equation 15 can be rewritten for oxygen and carbon dioxide as follows:

$$\int_{P_{v\text{O}_2}}^{P_{\text{O}_2}} \left( \frac{1}{P_{A\text{O}_2} - P_{\text{O}_2}} \right) dF_1(P_{\text{O}_2}, P_{\text{CO}_2}) = \beta K \left( \frac{A}{T_m \dot{Q}} \right) \frac{\alpha_{\text{O}_2} / P_B}{(\text{MW}_{\text{O}_2})^{1/2} (1 - \delta)} \quad (30)$$

and

$$\int_{P_{v\text{CO}_2}}^{P_{\text{CO}_2}} \left( \frac{1}{P_{A\text{CO}_2} - P_{\text{CO}_2}} \right) dF_2(P_{\text{CO}_2}, P_{\text{O}_2}) = \beta K \left( \frac{A}{T_m \dot{Q}} \right) \frac{\alpha_{\text{CO}_2} / P_B}{(\text{MW}_{\text{CO}_2})^{1/2} (1 - \delta)} \quad (31)$$

in which  $F_1(P_{\text{O}_2}, P_{\text{CO}_2})$  and  $F_2(P_{\text{CO}_2}, P_{\text{O}_2})$  are empirical expressions of the  $\text{O}_2$  and  $\text{CO}_2$  dissociation curves.

Similarly, for oxygen and carbon dioxide, equation 17 becomes

$$C_{aO_2} = (1 - \delta)F_1(P_{aO_2}^*, P_{aCO_2}^*) + \delta F_1(P_{vO_2}, P_{vCO_2}) \quad (32)$$

and

$$C_{aCO_2} = (1 - \delta)F_2(P_{aCO_2}^*, P_{aO_2}^*) + \delta F_2(P_{vCO_2}, P_{vO_2}). \quad (33)$$

Solution of equations 30, 31, 32, and 33 requires that the functions  $F_1(P_{O_2}, P_{CO_2})$  and  $F_2(P_{CO_2}, P_{O_2})$  be determined. The experimental data from which we will obtain these two unknown functions is that of Dill (1962). In this reference, volumes per cent is defined as the number of cc's of gas per 100 cc's of blood. Concentration as it appears in the preceding derivation is, therefore, equal to volumes per cent divided by one hundred.

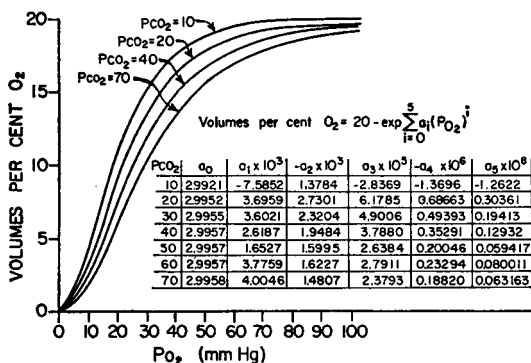


FIGURE 5 The oxygen dissociation curve for seven values of  $P_{CO_2}$ . Only four of the seven curves are shown.

The oxyhemoglobin dissociation curve can be fitted very accurately over the range 0-110 mm Hg by

$$\text{volumes per cent } O_2 = 20 - \exp \sum_{i=0}^5 a_i (P_{O_2})^i \quad (34)$$

in which  $a_0, \dots, a_5$  are functions of  $P_{CO_2}$ . Values of these parameters are shown in Fig. 5 for seven values of  $P_{CO_2}$  ranging from 10-70 mm Hg. Linear interpolation between sets of these seven curves will be used to obtain intermediate values of volumes per cent  $O_2$ .  $F_1(P_{O_2}, P_{CO_2})$  can be expressed, then as follows:

$$F_1(P_{O_2}, P_{CO_2}) = [20 - \exp \sum_{i=0}^5 a_i (P_{O_2})^i] / 100 + (P_{O_2} / P_B) \alpha_{O_2} = C_{O_2} \quad (35)$$

in which  $(P_{O_2} / P_B) \alpha_{O_2}$  is the dissolved  $O_2$  concentration.

The carbon dioxide dissociation curve can be fitted empirically by

$$\text{volumes per cent CO}_2 = \frac{aP_{\text{CO}_2} + b(P_{\text{CO}_2})^2}{1 + cP_{\text{CO}_2}} \quad (36)$$

in which  $a$ ,  $b$ , and  $c$  are functions of  $P_{\text{O}_2}$ . Values for these parameters are shown in Fig. 6 for six values of  $P_{\text{O}_2}$  ranging from 10–140 mm Hg. Again, linear interpolation will be used between curves.

$F_2(P_{\text{CO}_2}, P_{\text{O}_2})$ , therefore, becomes

$$F_2(P_{\text{CO}_2}, P_{\text{O}_2}) = \left[ \frac{aP_{\text{CO}_2} + b(P_{\text{CO}_2})^2}{1 + cP_{\text{CO}_2}} \right] / 100 = C_{\text{CO}_2}. \quad (37)$$

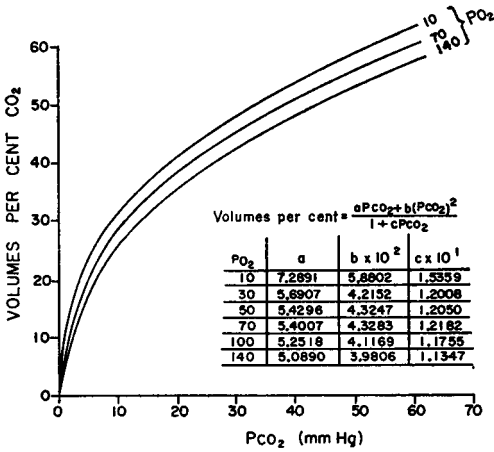


FIGURE 6 The carbon dioxide dissociation curve for six values of  $P_{\text{O}_2}$ . Only three of the six curves are shown.

Solution of equations 30, 31, 35, and 37 yields the partial pressure gradients for oxygen and carbon dioxide from the venous blood end of the pulmonary capillaries to the arterial blood end. These equations were solved by means of a digital computer program as follows: First, equations 30 and 31 were divided by their respective coefficients of  $\beta$  so that  $\beta$  alone remained on the right hand side of each equation.  $P_{\text{O}_2}$  in equation 30 was then incremented in steps of 0.1 mm Hg beginning with  $P_{\text{vO}_2}$ . An iterative procedure was then used to determine the  $P_{\text{CO}_2}$  value which caused the two computed values of  $\beta$  to fall within a preset tolerance of each other for each increment in  $P_{\text{O}_2}$ . This procedure was continued until  $\beta$  approached sufficiently close to 1.0.

Solution of equations 32, 33, 35, and 37 yields the arterial partial pressures resulting from venous admixture. These equations were solved for  $C_{\text{aO}_2}$  and  $C_{\text{aCO}_2}$  directly. Then, these values, along with the functions  $F_1(P_{\text{O}_2}, P_{\text{CO}_2})$  and  $F_2(P_{\text{CO}_2}, P_{\text{O}_2})$ , were used together in an iterative routine to determine  $P_{\text{aO}_2}$  and  $P_{\text{aCO}_2}$ .

Values of the parameters used for the normal case which have not already been given are as follow:

$$\begin{aligned}
 P_{A_{O_2}} &= 104 \text{ mm Hg} \\
 P_{v_{O_2}} &= 40 \text{ mm Hg} \\
 MW_{O_2} &= 0.032 \text{ kg} \\
 \alpha_{O_2} &= 0.022 \text{ atm}^{-1} \\
 \alpha_{CO_2} &= 0.510 \text{ atm}^{-1} \\
 P_{A_{CO_2}} &= 40 \text{ mm Hg} \\
 P_{v_{CO_2}} &= 46 \text{ mm Hg} \\
 MW_{CO_2} &= 0.044 \text{ kg} \\
 P_B &= 760 \text{ mm Hg}
 \end{aligned}$$

Solution of all six equations for the normal case as  $\beta$  is varied in increments between zero and unity is shown in Fig. 7. In this figure the results have been normalized. The difference between alveolar and capillary  $P_{O_2}$  is taken as ranging from zero to unity. To keep the direction of the gradient correct,  $P_{CO_2}$  has been normalized between zero and unity in the opposite direction (scale not shown). The solid ascending curve is the partial pressure gradient of oxygen. The concave shape between  $\beta = 0$  and  $\beta = 0.3$  can be explained by the convex shape of the oxygen dissociation curve above 40 mm Hg which reduces the partial pressure difference between alveolus and blood in this range and thereby reduces the rate of diffusion which would occur if a linear relation existed.

Calculation of the average partial pressure difference  $(\Delta P_{O_2})_{av}$  yields a value of 13 mm Hg. Multiplication of this value by the diffusing capacity upon which this curve was based yields an oxygen consumption  $\dot{V}_{O_2}$  of 273 cc/min/mm Hg which is in the normal range. This serves as a check on the validity of the curve.

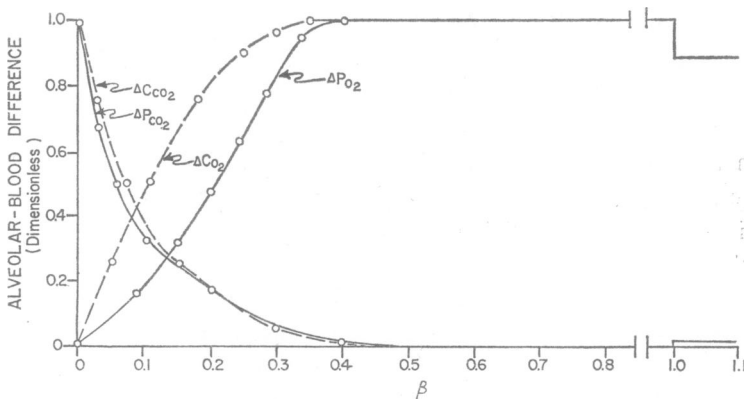


FIGURE 7 Normal oxygen and carbon dioxide partial pressure and concentration gradients along the pulmonary capillary pathway and venous admixture effects for  $P_{A_{O_2}} = 104$ ,  $P_{A_{CO_2}} = 40$ ,  $P_{v_{O_2}} = 40$ , and  $P_{v_{CO_2}} = 46$ .

The broken line ascending curve is the normal concentration gradient of oxygen along the capillary pathway. Note the absence of the concavity which appeared in the partial pressure gradient.

The descending solid curve of Fig. 7 is the normalized  $P_{\text{CO}_2}$  gradient as  $\beta$  is varied in increments from zero to unity. The most prominent thing about this curve is that equilibrium is not reached extremely rapidly as thought by some. Although  $\text{CO}_2$  does diffuse some twenty times as fast as oxygen, the blood can give up a larger quantity of  $\text{CO}_2$  per mm Hg change in partial pressure. This, coupled with the lower initial difference, prevents the gradient along the capillary path from changing twenty times as rapidly as that of oxygen. The validity of this curve can be checked as follows: Assuming a respiratory quotient  $RQ$  of 0.85, we obtain a carbon dioxide production rate  $\dot{V}_{\text{CO}_2}$  of 232 cc/min. Calculation of the average partial pressure difference  $(\Delta P_{\text{CO}_2})_{\text{av}}$  yields 0.566 mm Hg. Division of  $\dot{V}_{\text{CO}_2}$  by  $(\Delta P_{\text{CO}_2})_{\text{av}}$  yields a diffusing capacity for carbon dioxide  $D_{\text{CO}_2}$  of 410 cc/min/mm Hg which is in the normal range.

The validity of the gradient curves of Fig. 7 is further borne out by a theoretical analysis of Defares and Visser (1962) which yielded similar results when they divided the diffusing capacity of  $\text{O}_2$  into 100 equal segments and calculated the partial pressure gradients of oxygen and carbon dioxide for the normal case; i.e.,  $D_{\text{CO}_2} : D_{\text{O}_2} = 20:1$ , and the hypothetical cases of 10:1 and 40:1. "Physiological" dissociation curves were also determined for these cases. Similar results were also obtained by Milhorn (1966) in a much less extensive study than the present one in which the gradients for the normal case alone were investigated separately. In this study, assumed "physiological" dissociation curves were used so that coupling between sets of equations for  $\text{O}_2$  and  $\text{CO}_2$  was not involved. Furthermore, the experimental work of Craw et al. (1963) and Forster (1964) has indicated that, "If anything, the equilibration of  $\text{CO}_2$  with blood will be slower than that of  $\text{O}_2$ ." Examination of the  $P_{\text{O}_2}$  and  $P_{\text{CO}_2}$  gradients of Fig. 7 will show that the model does in fact predict that equilibration of alveolar  $P_{\text{CO}_2}$  with blood is slightly slower than that of oxygen.

The normal concentration gradient for carbon dioxide is given by the broken line descending curve of Fig. 7.

At the arterial blood end of the capillaries, the venous blood which has bypassed the capillaries by way of a-v shunts remixes to give a venous admixture drop in  $P_{\text{O}_2}$  of 7 mm Hg (Fig. 7), which is in good agreement with the experimental value of 7.3 mm Hg determined by Cole and Bishop (1963), and an increase in  $P_{\text{CO}_2}$  of 0.140 mm Hg (which may be considered negligible). These partial pressure changes correspond to concentration changes of 0.001 and 0.0006 for oxygen and carbon dioxide, respectively.

Fig. 8 shows the predicted "physiological" oxygen dissociation curve for the normal case. The numbers along the curve are the corresponding  $P_{\text{CO}_2}$  values.

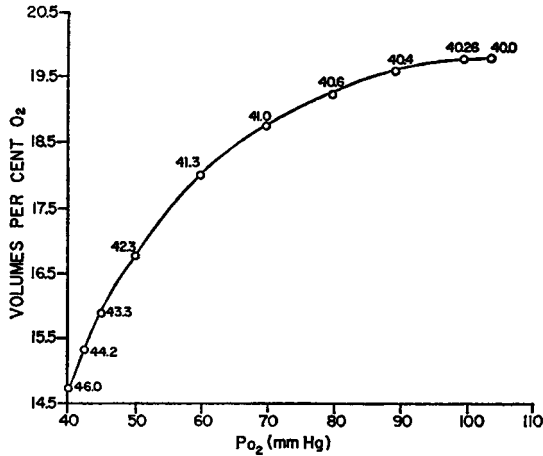


FIGURE 8 The theoretical physiological  $O_2$  dissociation curve.

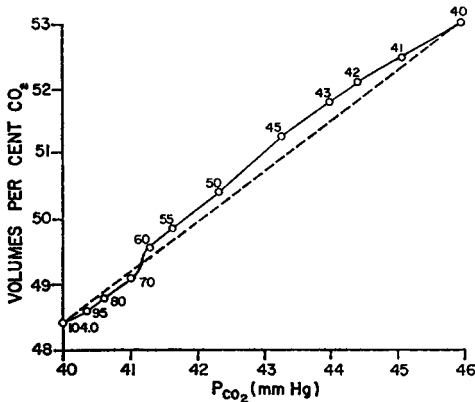


FIGURE 9 The theoretical physiological  $CO_2$  dissociation curve.

Fig. 9 shows the predicted "physiological" carbon dioxide dissociation curve for the normal case. The numbers along the curve are the corresponding  $P_{O_2}$  values. The broken straight line represents the "physiological" dissociation curve which is usually used without any real basis. The results shown in Figs. 8 and 9 are similar to those obtained by Defares and Visser in 1962.

The normalized effects on the  $P_{O_2}$  and  $P_{CO_2}$  gradients of alteration of the factor  $A/T_m\dot{Q}$  are shown in Fig. 10. The two solid curves (marked by the circles) are the predicted normal  $P_{O_2}$  and  $P_{CO_2}$  gradients redrawn from Fig. 7. The broken line curves to the right of these (marked by the triangles) are the predicted gradients for  $A/T_m\dot{Q}$  being one-half normal. This is equivalent in the physiological organism to (a) the pulmonary membrane surface area  $A$  being reduced to one-half of its normal value, corresponding to emphysema, (b) the pulmonary membrane being twice its



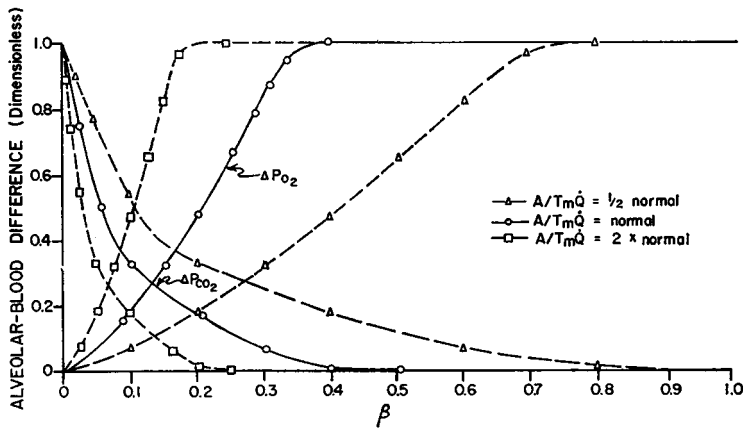


FIGURE 10 The effect of normal, one-half normal, and two times normal  $A/T_m\dot{Q}$  on the oxygen and carbon dioxide partial pressure gradients along the pulmonary capillary pathway for the constants given in Fig. 7.

normal thickness  $T_m$ , corresponding to pulmonary congestion, or (c) the cardiac output  $\dot{Q}$  being increased to twice normal output. The curves to the left of the normal curves (marked by the squares) are the predicted  $P_{O_2}$  and  $P_{CO_2}$  gradients for  $A/T_m\dot{Q}$  being two times normal. This could result from a decreased cardiac output corresponding to reduced cardiac function, or a greater than normal pulmonary membrane area, or reduced membrane thickness.

For the case of  $A/T_m\dot{Q}$  being one-half normal (Fig. 10), blood  $P_{CO_2}$  just barely reaches equilibrium with alveolar  $P_{CO_2}$  by the time the blood reaches the end of the capillary. This indicates that a combination of abnormal values for  $A$ ,  $T_m$ , and  $\dot{Q}$  could cause alveolar-blood partial pressure differences to develop at the end of the capillary for carbon dioxide as well as oxygen. This has been known to be true for oxygen for some time, but it has been thought by many that, because of the rapidity with which  $CO_2$  diffuses, blood  $P_{CO_2}$  invariably reaches equilibrium with alveolar  $P_{CO_2}$  before leaving the pulmonary capillary. Apparently, this may not always be true.

Concentration gradients are shown in Fig. 11 for  $A/T_m\dot{Q}$  being one-half normal (marked by the triangles), normal (marked by the circles) and twice normal (marked by the squares).

The effect of breathing 10% oxygen on the partial pressure gradients are shown in Fig. 12. Again, the results have been normalized, so that zero corresponds to 25 mm Hg and unity corresponds to 40 mm Hg for oxygen. For carbon dioxide, zero corresponds to 30 mm Hg and unity corresponds to 35 mm Hg. The ratio of surface area  $A$  to cardiac output  $\dot{Q}$  has been reduced by 20% for this case. The oxygen gradient for the normal situation (marked by the circles) is seen to rise to a maximum of 33.1 mm Hg which means that a diffusion difference of 6.9 mm Hg exists between alveolar  $P_{O_2}$  and end capillary  $P_{O_2}$ . In addition to this, venous admixture adds

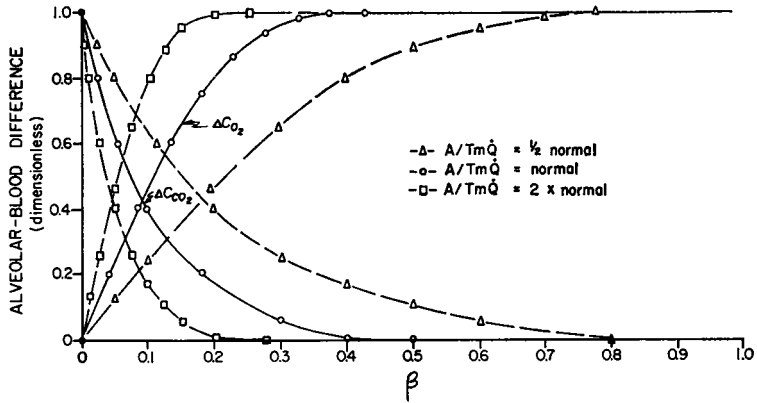


FIGURE 11 The effect of normal, one-half normal, and two times normal  $A/T_m\dot{Q}$  on the concentration gradients of oxygen and carbon dioxide along the pulmonary capillary pathway for the constants given in Fig. 7.

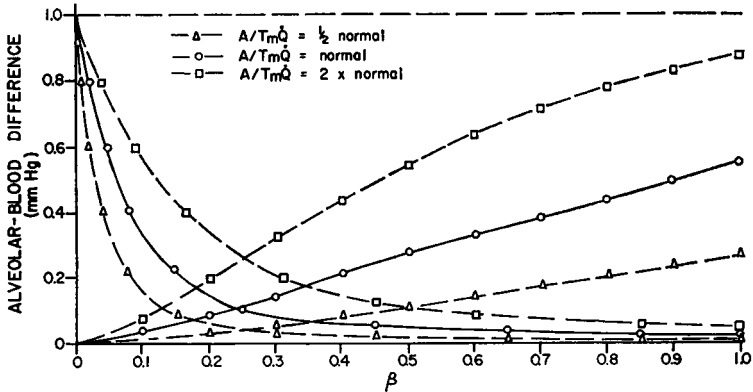


FIGURE 12 The effect of breathing 10% oxygen on the oxygen and carbon dioxide partial pressure gradients along the pulmonary capillary pathway for normal, one-half normal, and two times normal  $A/T_m\dot{Q}$ .  $P_{A_{O_2}} = 40$ ,  $P_{A_{CO_2}} = 30$ ,  $P_{v_{O_2}} = 25$ , and  $P_{v_{CO_2}} = 35$ .

another 0.22 mm Hg difference, giving a total of 7.12 mm Hg between alveolar gas and arterial gas. This is in agreement with Lilienthal et al. (1946) who showed that breathing low oxygen caused only a slight change from normal in the alveolar-arterial difference. The effect of  $A/T_m\dot{Q}$  being one-half normal is marked by the squares and the effect of  $A/T_m\dot{Q}$  being two times normal is marked by the triangles.

The carbon dioxide partial pressure gradient for normal  $A/T_m\dot{Q}$  is shown by the descending curve marked with the circles. The effect of  $A/T_m\dot{Q}$  being one-half normal is marked with the triangles and the effect of  $A/T_m\dot{Q}$  being two times normal is marked with the squares. It should be noted that diffusion differences between alveoli and end-capillary blood do exist, although they are small. Combinations of

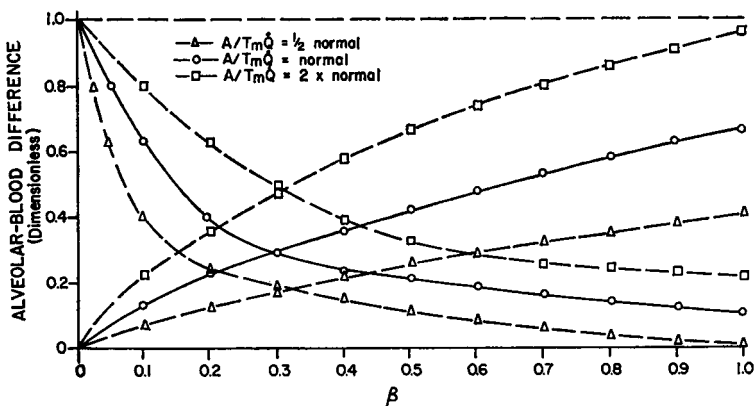


FIGURE 13 The effect of breathing 10% oxygen on the oxygen and carbon dioxide concentration gradients along the pulmonary capillary pathway for normal, one-half normal, and two times normal  $A/T_m\dot{Q}$  and the constants given in Fig. 12.

abnormal values of  $A$ ,  $T_m$ , and  $\dot{Q}$  could, in theory, cause larger and possibly significant differences.

Normalized concentration gradients are shown in Fig. 13. For oxygen, unity corresponds to 0.156 and zero to 0.103. For carbon dioxide, unity corresponds to 0.490 and zero to 0.446.

### INCORPORATION INTO A COMPLETE RESPIRATORY SYSTEM MODEL

As mentioned previously, the objective of this study has been to develop a model of pulmonary capillary gas exchange and venous admixture which could later be incorporated into a model of the complete respiratory system. In this section we will discuss how this could be done. Fig. 14 shows a simplified block diagram of the respiratory system. The center block represents the alveolar model, the lower block represents the capillary gas exchange and venous admixture model (with  $\beta = 1.0$ ) which was developed in the present study, and the upper block represents the rest of the respiratory system model whose details are not pertinent to this discussion. It is sufficient to say that the latter block contains all of the tissues, the circulatory controller which determines cardiac output, and the ventilatory controller which determines alveolar ventilation. Inputs to the alveolar model are alveolar ventilation  $\dot{V}_A$ , inspired  $O_2$  partial pressure  $P_{IO_2}$ , inspired  $CO_2$  partial pressure  $P_{ICO_2}$ , and the end capillary partial pressures  $P_{aO_2}^*$  and  $P_{aCO_2}^*$ . These inputs determine the alveolar partial pressures  $P_{AO_2}$  and  $P_{ACO_2}$  which become the inputs to the lower block, along with cardiac output  $\dot{Q}$  and the mixed venous partial pressures  $P_{vO_2}$  and  $P_{vCO_2}$ . Outputs of this block are the end capillary partial pressures  $P_{eO_2}^*$  and  $P_{eCO_2}^*$  which are inputs to the alveolar model, and the arterial partial pressures  $P_{aO_2}$  and  $P_{aCO_2}$  which are the inputs to the upper block. It is these inputs to the upper block, along with the

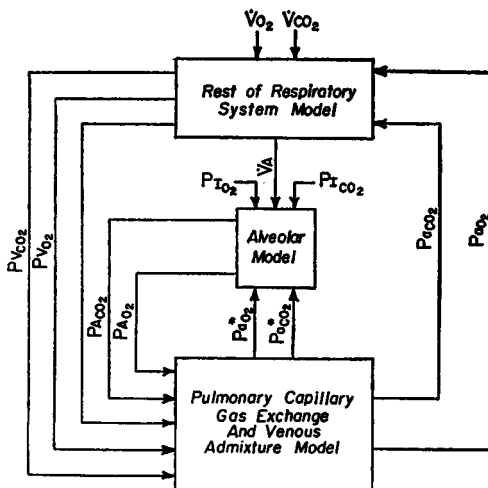


FIGURE 14 A simplified block diagram of the human respiratory system which includes the pulmonary capillary gas exchange and venous admixture model.

rate of oxygen consumption  $\dot{V}_{O_2}$  and  $CO_2$  production  $\dot{V}_{CO_2}$ , which determine alveolar ventilation  $\dot{V}_A$  and cardiac output  $\dot{Q}$ , as well as the venous partial pressures  $P_{vO_2}$  and  $P_{vCO_2}$ .

Because the transit time of blood through the pulmonary capillaries is short (Roughton, 1945) compared to the time constants of changes in alveolar and arterial blood partial pressures, it is assumed to be instantaneous. New values for  $P^*_{O_2}$ ,  $P^*_{CO_2}$ ,  $P_{aO_2}$ , and  $P_{aCO_2}$  are, therefore, calculated for each iteration in the over-all respiratory system model. Development of this over-all respiratory system model is presently in progress.

### SUMMARY AND DISCUSSION

The development of a digital computer model of pulmonary capillary gas exchange and venous admixture has been presented. The model has been used to predict partial pressure and concentration gradients along the pulmonary capillary pathway of helium, nitrogen, oxygen, and carbon dioxide. These studies were done in two groups. First, the linear case of nitrogen and helium was studied. This case is simpler than the nonlinear case of oxygen and carbon dioxide because (a) inert gases obey Henry's law in blood which is linear and (b) there is no coupling between gases. This study has predicted that capillary blood  $N_2$  and  $He_2$  reach equilibrium extremely rapidly and that very minute concentration changes in blood cause very large partial pressure changes.

The nonlinear case of oxygen and carbon dioxide is more difficult to study because (a) the dissociation curves of oxygen and carbon dioxide are nonlinear and (b) oxygen and carbon dioxide are coupled in blood by the Bohr and Haldane effects. The nonlinear case has been studied for breathing room air (the normal case) and breathing 10% oxygen. The study of the normal case has predicted several things of interest as follow: First, the partial pressure of blood reaches equilibrium with

alveolar oxygen at about two-fifths of the way along the capillary pathway. Carbon dioxide reaches equilibrium slightly later at about the middle of the capillary. Secondly, the partial pressure gradient of oxygen has a concave shape due to the convex shape of the oxygen dissociation curve. This concavity is absent in the concentration gradient of oxygen and in both the partial pressure and concentration gradients of carbon dioxide. The slow change in the blood partial pressure of carbon dioxide has indicated that in certain disease conditions in which combinations of altered membrane surface area, membrane thickness, and cardiac output occur, differences between alveolar  $P_{CO_2}$  and end capillary  $P_{CO_2}$  may occur. Small differences do, in fact, occur while breathing low oxygen concentrations.

The present study, although a simplification of the actual system, has been very informative, and has yielded results which agree well with the small amount of data present in the literature. The areas of simplification are as follows: (a) The capillary system has been considered to consist of a parallel network whereas, in truth, it is a hexagonal mesh network. The mesh is so small that the capillary bed is considered by many as a thin sheet of blood. Hence, a parallel network is probably a justifiable assumption. (b) Because of the complexity and dubious effects introduced by including axial diffusion in the model, it has not been included. (c) The lungs have been considered to be in a static state; i.e., the studies of this paper are considered to take place at the end of inspiration or the end of expiration. Effects of respiration are left for future studies.

This work was supported by a Public Health Service grant-in-aid.

Received for publication 13 October 1967 and in revised form 15 December 1967.

## REFERENCES

- COLE, R. B., AND J. M. BISHOP. 1963. *J. Appl. Physiol.* 18:1043.
- CRAW, M., H. P. CONSTANTINE, J. A. MORELLO, AND R. E. FORSTER. 1963. *J. Appl. Physiol.* 18:317.
- DEFARES, J. G., H. E. DERKSON, AND J. W. DUYFF. 1960. *Acta Physiol. Pharmacol. Neerl.* 9:327.
- DEFARES, J. G., AND B. F. VISSER. 1962. *Ann. N. Y. Acad. Sci.* 96:939.
- DILL, D. B., H. J. EDWARDS, AND W. V. CONSOLAZIO. 1962. *In A Graphical Analysis of Respiratory Gas Exchange.* H. Rahn and W. Fenn. The American Physiological Society, Washington, D.C.
- FORSTER, R. E. 1964. *In Handbook of Physiology.* W. O. Fenn and H. Rahn, editors. American Physiological Society, Washington, D. C. Vol. I.
- GRODINS, F. S., J. S. GRAY, K. R. SCHROEDER, A. L. NORINS, AND R. W. JONES. 1954. *J. Appl. Physiol.* 7:283.
- HORGAN, J. D., AND R. L. LANGE. 1962. *Proc. 15th Ann. Conf. Eng. in Med. Biol.* 4:53.
- LILIENTHAL, J. L., JR., R. L. RILEY, D. D. PROMMET, AND R. E. FRANKE. 1946. *Am. J. Physiol.* 147:199.
- LONGOBARDO, G. S., N. S. CHERNIACK, AND A. P. FISHMAN. 1966. *J. Appl. Physiol.* 21:1839.
- MILHORN, H. T., JR. 1966. *Proc. 4th Ann. Symp. Biomath. Computer Sci. Life Sciences.* 14.
- MILHORN, H. T., JR., R. BENTON, R. ROSS, AND A. C. GUYTON. 1965. *Biophys. J.* 5:27.
- MILHORN, H. T., JR., AND A. C. GUYTON. 1965. *J. Appl. Physiol.* 20:328.
- MILHORN, H. T., JR., A. C. GUYTON, AND T. G. COLEMAN. 1967. *Proc. 61st Ann. AIChE Conf. Session* 34. 1.
- ROUGHTON, F. J. W. 1945. *Am. J. Physiol.* 143:621.
- WEIBEL, E. R., AND D. M. GOMEZ. 1962. *Science.* 137:577.